Stochastic Multistage Coplanning of Transmission Expansion and Energy Storage

Ting Qiu, *Student Member, IEEE*, Bolun Xu, *Student Member, IEEE*, Yishen Wang, *Student Member, IEEE*, Yury Dvorkin, *Student Member, IEEE*, and Daniel S. Kirschen, *Fellow, IEEE*

***Abstract*—Transmission expansion and energy storage increase the flexibility of power systems and, hence, their ability to deal with uncertainty. Transmission lines have a longer lifetime and a more predictable performance than energy storage, but they require a very large initial investment. While battery energy storage systems (BESS) can be built faster and their capacity can be increased gradually, their useful life is shorter because their energy capacity degrades with time and each charge and discharge cycle. Additional factors, such as the expected profiles of load and renewable generation significantly affect planning decisions. This paper proposes a stochastic, multistage, coplanning model of transmission expansion, and BESS that considers both the delays in transmission expansion and the degradation in storage capacity under different renewable generation and load increase scenarios. The proposed model is tested using a modified version of the IEEE-RTS. Sensitivity analyses are performed to assess how factors such as the planning method, the storage chemistry characteristics, the current transmission capacity, and the uncertainty on future renewable generation and load profiles affect the investment decisions.**

***Index Terms*—Battery degradation, battery energy storage, stochastic optimization, transmission expansion, uncertainty.**

NOMENCLATURE

Sets and Indices

y	Index to the study year, from 1 to y.
t	Index to the time interval, from 1 to T.
i	Index to the generators, from 1 to I.
b	Index to the piece-wise linear cost segment, from 1 to NB.
l	Index to the transmission lines, from 1 to L.
s	Index to the nodes, from 1 to S.
w	Index to the wind farms, from 1 to W.

Parameters

τ	Number of days represented by each typical day in a year.
r	Discount rate.
ST	Life time of a BESS.
LT	Life time of a transmission line.
$k_{i,b}$	Marginal cost of a segment of generator cost curve.
C^e	Cost per MWh of a BESS.
C^p	Cost per MW of a BESS.
C^l	Cost per MW of capacity of a transmission line.
k^e	Annualized cost per MWh of a BESS.
k^p	Annualized cost per MW of a BESS.
k^l	Annualized cost per MW of a transmission line.
NL_i	No-load cost of a generator.
Δ_i	Generator ramp rate.
$\bar{p}_{i,b}$	Maximum generation of each segment of a cost curve.
$\underline{p}_i$, $\bar{p}_i$	Minimum and maximum generation of each generator.
δt	Spinning reserve response time.
η_s^{dis}, η_s^{ch}	Storage device discharge and charge efficiency.
$E_s^{\min}$	Minimum energy capacity of a BESS.
$wf_{w,t}^y$	Wind forecast.
$D_{s,t}^y$	Load forecast.
$\bar{F}_{l,t}$	Transmission line rating.
$M_{i,s}^G$	Mapping of generators to nodes.
$M_{w,s}^W$	Mapping of wind farms to nodes.
$M_{l,s}^L$	Line connection.
B_{ms} B	Matrix for dc power flow calculation.
r_s	Energy capacity degradation factor of energy storage.
k_{cal}	Calendar ageing rate.
k_{cycle}	Cycling ageing rate.

Binary variables

$x_{i,t}^y$	Generator status, 1- online, 0 - offline.
$I_{l,y}$	Line decision, 1- start construction, 0 - no construction.
$Z_{l,y}$	New line status, 1- in service, 0 - not in service.

Variables

C_y	Discounted annual operation cost.
$C_{t,i}^{\text{operation}}$	Hourly unit operation cost.
S_INV_y	Discounted annual storage investment cost.
L_INV_y	Discounted annual line investment cost.
$p_{i,b,t}^y$	Generation on each segment of the cost curve.
$p_{i,t}^y$	Total generation of each generator.
$ch_{s,t}^y$	Charging power of a BESS.
$dis_{s,t}^y$	Discharging power of a BESS.
$SoC_{s,t}^y$	State of charge of a BESS.
$\theta_{s,t}^y$	Bus voltage angle.

I. INTRODUCTION

LARGER proportions of stochastic renewable energy sources, such as wind and solar, further increase the uncertainty affecting the system. Dealing effectively with more uncertainty requires more flexibility. In the short-term,

Manuscript received November 5, 2015; revised March 7, 2016; accepted April 3, 2016. Date of publication April 20, 2016; date of current version December 20, 2016. Paper no. TPWRS-01850-2015.

The authors are with the Department of Electrical Engineering, University of Washington, Seattle, WA 98105 USA (e-mail: tqiu@uw.edu; xubolun@uw.edu; ywang11@u.washington.edu; dvorkin@uw.edu; kirschen@uw.edu).

Color versions of one or more of the figures in this paper are available online at http://ieeexplore.ieee.org.

Digital Object Identifier 10.1109/TPWRS.2016.2553678

operational time frame, this can be achieved using advanced optimization techniques (such as stochastic optimization, interval optimization or robust optimization [1]–[5]), by implementing a rolling unit commitment (UC) horizon [6], [7], or simply increasing the reserve requirements [8]–[12]. Over a longer, planning timeframe, one should consider deploying flexible resources such as energy storage systems and/or expanding the generation and transmission capacity. Since the cost of building storage and transmission capacity is high and the risk associated with stranded investments is significant, it is essential to develop techniques that will determine the right balance between these resources and ensure that the solution is robust to the inevitable long term forecasting errors.

Generation and transmission planning have been extensively studied in the literature. Hemmati *et al*. [13] provide a comprehensive review of the topic while Munoz *et al*. [14] and Martinez Cesena *et al*. [15] discuss recent progress. With the development of battery technologies, the combined operation and planning of storage devices with other power system resources is drawing increasing attention. Zach and Auer [16] point out that energy storage and transmission investments increase system flexibility but that cost/benefit analyses are needed to determine which measures are preferable.

Various studies [17]–[23] focus on the planning of energy storage systems alone in power systems. A DCOPF model is used in Oh [17], and a limited number of time periods per year are considered to make the problem of siting and sizing storage units tractable. A full unit commit model is used in Pandzic *et al*. [18] to determine both the optimal sizes and sites for energy storage using wind and load profile over a whole year, and some heuristics are introduced to limit the problem size. Other authors [19]–[21] focus on the size of energy storage without considering the effects of the transmission network. The statistical properties of renewable generation are used in Liu *et al*. [19], and the power spectrum density of deviations of renewable generation from forecasts is applied in Li *et al*. [20]. Bayram *et al*. [21] developed a stochastic analytical framework to determine the proper size of energy storage, and conducted a benefit/cost analysis to evaluate storage investments.

Co-planning of energy storage and transmission systems is addressed in [22]–[25]. Hu *et al*. [22] solve a MILP problem iteratively to determine the ESS investment size and locations by replacing part of the transmission investment while satisfying the same system requirement. Zhang *et al*. [23] propose a MILP model to determine the size and location of a single energy storage unit to minimize both the operation and investment costs taking line losses into account. Hedayati *et al*. [24] and Konstantelos and Strbac [25] propose multi-stage co-planning models to determine the location of a given size energy storage that minimizes the one-time investment cost and the long term operation cost. A DCOPF based deterministic planning model is used in Hedayati *et al*. [24], while a SCOPF based stochastic planning framework is used. This latter work Konstantelos and Strbac [25] takes into account N-1 security criteria as well as the uncertainty on the long term wind capacity.

This paper describes a more accurate technique for co-planning the multi-stage expansion of transmission capacity and the deployment of battery energy storage systems (BESS). Its contributions can be summarized as follows:

1) It models the degradation in energy storage capacity due to shelf life and charge/discharge cycles.
2) It accounts for the delays associated with the planning and construction of transmission lines.
3) It incorporates a UC with reserve requirements to represent accurately the operation of the system
4) It optimizes both the size and the location of investments in energy storage at each year of the horizon.
5) It implements a stochastic optimization to take into account the effect of uncertainty on load as well as renewable generation.

The rest of the paper is organized as follows. Section II describes the modeling assumptions while Section III provides the detailed mathematical formulation of the optimization problem. Section IV describes the test system. Section V presents the results of the optimization and of the sensitivity analysis. Section VI concludes.

II. Modeling

Multi-stage planning problems can easily get very large. Careful choices about modeling assumptions must therefore be made to achieve a balance between the accuracy of the results and the computing time.

A. Battery Energy Storage Systems

The calendar life of a battery as well as the charge and discharge cycles it has undergone affect its energy capacity. A number of papers [26]–[28] offer detailed and accurate models of battery degradation. However, because these models are non-linear and involve multiple variables and non-linearity, the computational burden that they would impose on a planning study is not acceptable. In this paper, we assume instead a flat degradation rate of 94%, which means that 6% of the energy capacity is lost each year, 3% of which is due to calendar aging and 3% to utilization.

Energy storage planning techniques described in the literature (e.g., [18]–[25]) typically determine the optimal location for storage unit of a given size and for a one-time investment. This is a rather restrictive assumption as storage lends itself to incremental investments over time at the same location. Instead, we assume as shown in Fig. 1, that BESS units can be added over time at each location, providing a variable power/energy capacity ratio. Each BESS unit is retired independently when it reaches the end of its useful life.

B. System Operation

Enhancing the fidelity of the modeling of system operation increases the numbers of variables and constraints. In a planning model, these numbers increase further as the number of years considered as part of the planning horizon is extended. Different strategies have been used to streamline the operation model. Most planning models ignore or simplify the UC decisions and constraints or use very broad time periods. Konstantelos and

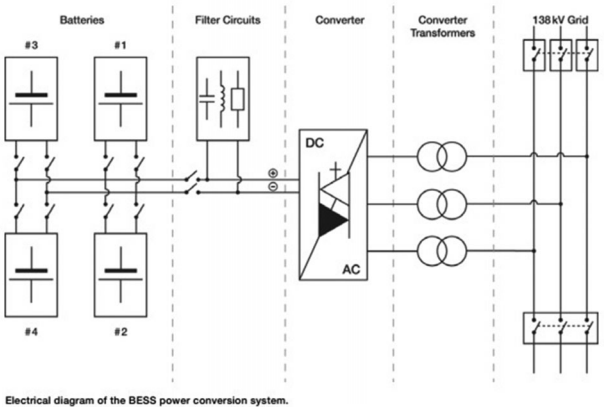

Fig. 1. BESS investment unit [29].

Strbac [25] removed all time coupling constraints (such as the ramp rate limits on the generators), and considered a 15-year planning horizon with a 5-year epoch. Hedayati *et al*. [24] ignore the uncertainty on future wind generation and load and consider an eight-year horizon with a four-year epoch. These assumptions have serious drawbacks. First, it is impossible to know in advance which generating units will be committed under the current market structure. In particular, it is quite unlikely that all the intermediate and peaking units will be online at all times. The contribution of storage in dealing with the uncertainty in renewable generation and in reducing the number of start-ups of peaking units would therefore be undervalued. Second, because the available capacity of an energy storage system is likely to fade substantially over a five or eight year timeframe, using such a long planning epoch could lead to inaccurate planning decisions.

This paper adopts a 25-year planning horizon with a one-year epoch. To reduce the number of binary variables used to reflect the generators' status, all generators are divided into two types: those that are assumed to be always committed and those that are free, i.e., which can start up or shut down at any time. In other words, slow and fast generators. In this paper, generators with a one-hour minimum up/down time can be assumed to be fast generators, while the remaining ones are the slow category.

C. Reserve Requirement

Most planning models do not consider the need to provide operating reserve. As the proportion of stochastic renewable generation increases, this simplification becomes untenable. The proposed models considers the reserve constraint in the UC and uses the $3 + 5$ rule to specify the amount of operating reserve, this means that the reserve required is equal to 3% of the forecast load prediction plus 5% of the forecast wind generation [9], [30]. The amount of reserve provided by BESS follows the model described of Hu *et al*. [31].

D. Locations for BESS and Additional Transmission Capacity

Limiting the number of locations where BESS could be installed and the number of transmission lines that could be upgraded significantly reduces the computational burden. To determine a good set of likely candidates, a planning problem with one-year horizon was run to determine the best locations for each of the 25 years in the actual horizon. Locations where this short-term planning frequently installed BESS were selected as candidates for the long term planning problem. Lines where the power flow frequently exceeded 55% of their rating were considered for a capacity upgrade.

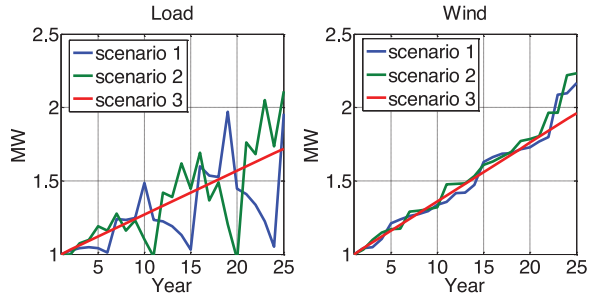

Fig. 2. Load and wind generation capacity scenarios.

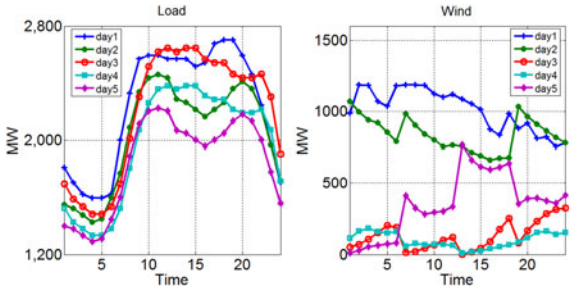

Fig. 3. Total load and wind generation of each representative day.

E. Load and Wind Generation Capacity Scenarios

To reduce the risk of stranded assets, investments in transmission or storage capacity should be robust with respects to errors in the long-term evolution of the load and the renewable generation capacity. The proposed optimal co-planning approach therefore considers three scenarios that combine the load and wind generation uncertainty as in Fig. 2.

F. Representative Days

In long term planning, considering a whole year of operation is unnecessary and makes the problem intractable. When integrating renewables, the shape of the net load can be quite different from the profile of the actual load. Thus, five days are selected to represent typical wind generation and load profiles for each year based on how the daily wind is changing with daily load as shown in Fig. 3.

A correlation coefficient is used to quantify the relation between daily load profiles and the wind generation profiles. In some cases these two profiles are positively correlated and in other cases they are anti-correlated. Together these profiles define the shape of the net load which drives the investment decisions. Since this correlation coefficient is independent of the load value and wind capacity which change over the years, we deem it a better feature to be used in the K-means algorithm

which selects the five representative days. The profile which is closest to the centroid of each cluster are selected as representative of that cluster. Since these five days are usually not consecutive, the initial ramp constraints are relaxed.

III. Formulation of the Planning Problem

A. Objective Function

For clarity of exposition, the equations below define the deterministic long-term planning problem, and the stochastic one can be easily get by adding one more dimension into the operation variable and related constraints. Equation (1) shows that the long-term planning problem aims to minimize the sum of the operating cost over the horizon:

$$\min \sum_{y=1}^{Y} C_y + S\_INV_y + L\_INV_y. \tag{1}$$

Equation (2) gives the discounted annual total operating cost over the planning horizon. The penalty term discourages wind curtailments (at 20 \$/MW · h) and load curtailments (at 5000 \$/MW·h)

$$C_y = \frac{\tau \cdot \left(\sum_{i=1,t=1}^{I,T} C_{t,i}^{\text{operation}} + \text{penalty}\right)}{(1+r)^{y-1}} \tag{2}$$

$$C_{t,i}^{\text{operation}} = \sum_{b=1}^{NB} p_{i,b,t}^{y} \cdot k_{i,b} + NL_i + SU_i \cdot x_{i,t}^{y}. \tag{2a}$$

Equation (3) gives the discounted BESS investment cost for each year. Equations (3a) and (3b) give the annualized BESS energy and power capacity cost while (3c) gives the annual discount factor needed to ensure that all costs are be paid off within the BESS life time

$$S\_INV_y = \sum_{n=1}^{y} \alpha_{y-n+1} \cdot \sum_{s=1}^{S} \left(k^e \cdot E_{s,n}^{\max} + k^p \cdot P_{s,n}^{\max}\right) \tag{2}$$

$$k^e = C^E \cdot \frac{r(1+r)^{ST}}{(1+r)^{ST}-1} \ (\$/\text{MW} \cdot \text{h} \cdot \text{Year}) \tag{3a}$$

$$k^p = C^p \cdot \frac{r(1+r)^{ST}}{(1+r)^{ST}-1} \ (\$/\text{MW} \cdot \text{Year}) \tag{3b}$$

$$\alpha_n = \begin{cases} \dfrac{1}{(1+r)^{n-1}} & n \le ST \\ 0 & n \ge ST+1 \end{cases}. \tag{3c}$$

Equation (4) gives the discounted transmission line investment cost for each year. An annual payment is assumed to be made each year after the investment decision is made. Equation (4a) gives the annualized line capacity cost while Equation (4b) gives the annual discount factor needed to ensure that the cost of the line is paid off over the line's life time

$$L\_INV_y = \sum_{n=1}^{y} \beta_{y-n+1} \cdot \sum_{l=1}^{L} k^l \cdot I_{l,n} \tag{4}$$

$$k^l = C^L \cdot \frac{r(1+r)^{LT}}{(1+r)^{LT}-1} \ (\$/\text{Year}) \tag{4a}$$

$$\beta_n = \begin{cases} \dfrac{1}{(1+r)^{n-1}} & n \le LT \\ 0 & n \ge LT+1 \end{cases}. \tag{4b}$$

B. Generator Constraints

Equations (5) to (8) implement the constraints on minimum and maximum generation capacity and maximum ramping

$$p_{i,t}^{y} = \sum_{b=1}^{NB} p_{i,b,t}^{y} \cdot x_{i,t}^{y} \tag{5}$$

$$p_{i,t}^{y} \ge \underline{p}_i \cdot x_{i,t}^{y} \tag{6}$$

$$p_{i,b,t}^{y} \le \bar{p}_{i,b} \cdot x_{i,t}^{y} \tag{7}$$

$$\left|p_{i,t}^{y} - p_{i,t-1}^{y}\right| \le \Delta_i. \tag{8}$$

C. Reserve Constraints

Equations (9) and (10) determine the amount of reserve that each generator can provide:

$$p_{i,t}^{y} + rg_{i,t}^{y} \le \bar{p}_i \cdot x_{i,t}^{y} \tag{9}$$

$$rg_{i,t}^{y} \le \Delta_i \cdot \delta t \cdot x_{i,t}^{y}. \tag{10}$$

D. Energy Storage Constraints

Equation (11) keeps track of the state of charge of each BESS while Equations (12) to (14) enforce their energy and power capacity limits. Equations (15) and (16) determine the amount of reserve that each BESS can provide:

$$SoC_{s,t}^{y} = SoC_{s,t-1}^{y} + ch_{s,t}^{y} - dis_{s,t}^{y} \tag{11}$$

$$E_{s,y}^{\min} \le SoC_{s,t}^{y} \le AE_{s,y} \tag{12}$$

$$ch_{s,t}^{y} \le APe_{s,y} \tag{13}$$

$$dis_{s,t}^{y} \le APe_{s,y} \tag{14}$$

$$0 \le re_{s,t}^{y} + dis_{s,t}^{y} - ch_{s,t}^{y} \le APe_{s}^{y} \tag{15}$$

$$E_{s}^{\min} \le SoC_{s,t}^{y} - \frac{\left(re_{s,t}^{y} - ch_{s,t}^{y}\right)}{\eta_s^{ch}} \cdot \delta t. \tag{16}$$

E. Power Balance Constraints

Equation (17) enforces the system power balance at each node. Equation (18) limits the wind generation to the availability of wind power, which is assumed to be equal to the forecast:

$$\sum_{i=1}^{I} p_{i,t}^{y} \cdot M_{i,s}^{G} - \sum_{w=1}^{W} wp_{w,t}^{y} \cdot M_{w,s}^{W} - \sum_{l=1}^{L} \left(f_{l,t}^{y} + N f_{l,t}^{y}\right) \cdot M_{l,s}^{L} = D_{s,t}^{y} + \sum_{t=1}^{T} \left(\frac{ch_{s,t}^{y}}{\eta_s^{ch}} + dis_{s,t}^{y} \cdot \eta_s^{dis}\right) \tag{17}$$

$$wp_{w,t}^{y} + ws_{w,t}^{y} = wf_{w,t}^{y}. \tag{18}$$

F. Reserve Requirement

Equation (18) defines the 3 + 5 reserve requirement [9], [30]. The total reserve should be no less than 3% of the forecasted load plus 5% of the forecasted wind power.

$$\sum_{i=1}^{I} rg_{i,t}^{y} + \sum_{s=1}^{S} re_{s,t}^{y} \geq 0.03 \cdot \sum_{s=1}^{S} D_{s,t}^{y} + 0.05 \cdot \sum_{w=1}^{W} wf_{w,t}^{y}. \tag{19}$$

G. Line Flows and Transmission Capacity

Equation (20) calculates the dc line power flows. Equations (21) and (22) implement the line flow constraints

$$f_{l,t}^{y} = B_{ms} \cdot \left(\theta_{m,t}^{y} - \theta_{s,t}^{y}\right) \tag{20}$$

$$-\bar{F}_{l,t} \leq f_{l,t}^{y} \leq \bar{F}_{l,t} \tag{21}$$

$$-\pi \leq \theta_{s,t}^{y} \leq \pi. \tag{22}$$

H. Storage Planning

Equation (23) gives the available BESS energy capacity for each year considering degradation. Equations (23a) and (23b) calculate the capacity factor at each year by combining the calendar aging and the aging caused by cycling. The energy capacity of a BESS is assumed to be zero once it reaches the end of its life

$$AE_{s,y} = \sum_{t_0=1}^{y} a_{y-t_0+1} \cdot E_{s,t_0} \tag{23}$$

$$a_n = \begin{cases} 1 \cdot CF^{n-1} & n \leq ST \\ 0 & n \geq ST+1 \end{cases} \tag{23a}$$

$$CF = 1 - k_{cal} - k_{cycle}. \tag{23b}$$

Equation (24) gives the available power capacity of a BESS for each year. No degradation is assumed. Equation (24a) removes this power capacity once the BESS has reached the end of its life

$$APe_{s,y} = \sum_{t_0=1}^{y} b_{y-t_0+1} \cdot Pe_{s,t_0} \tag{24}$$

$$b_n = \begin{cases} 1 & n \leq ST \\ 0 & n \geq ST+1 \end{cases}. \tag{24a}$$

Equations (25), (26) are optional constraints which specify that a certain amount of energy storage is available in a certain year

$$\sum_{s=1}^{S} AE_{s,y} = AE^{*} \tag{25}$$

$$\sum_{s=1}^{S} APe_{s,y} = APe^{*}. \tag{26}$$

Equation (27) keeps the power/energy capacity ratio of each BESS within a technologically reasonable range:

$$0.25 \leq \frac{Pe_{s,y}}{E_{s,y}} \leq 8. \tag{27}$$

I. Line Planning and Operation Model

Equation (28) record the year when a line is constructed, which triggers the investment cost in equation (4). Equations (28), (29) enforces a construction delay of one year between the investment decision and the availability of an expanded line. Equations (30), (31) determine the flows on new transmission lines

$$Z_{l,y} = \sum_{r=1}^{y-1} I_{l,r} \tag{28}$$

$$Z_{l,y} \geq Z_{l,y-1} \tag{29}$$

$$Nf_{l,t}^{y} = B_{mn} \cdot \left(\theta_{m,t}^{y} - \theta_{n,t}^{y}\right) \tag{30}$$

$$-\bar{F}_{l,t} \cdot Z_{l,y} \leq Nf_{l,t}^{y} \leq \bar{F}_{l,t} \cdot Z_{l,y}. \tag{31}$$

IV. Test System

Tests were carried out on a modified version of the IEEE-RTS 24-bus system. Full system data can be downloaded from [32]. The wind power profile used are from Pandzic *et al*. [18]. Only the three wind farms located at bus 20, 21 and 23 of subsystem 1 are selected with initial capacities of 600, 300 and 300 MW. Wind energy generation accounts for 21.7% of the annual load at year 1. A line was added between buses 7 and 8 to make the system N-1 secure. Other important testing parameters include:

1) Transmission capacity was reduced to 90% of its original.
2) The cost of a BESS is assumed to be 500 $/KW plus 25 $/KW · h, and its lifetime is assumed to be 10 years.
3) The cost of building a line is assumed to be 927 000 $ per line, and its lifetime is assumed to be 60 years [33].
4) The discount rate was set at 5%.
5) In the base scenario, the wind generation capacity increases linearly by 4% of the initial per year and the load by 3% of the initial value per year.
6) Buses candidates for BESS installations and lines candidates for transmission upgrades were selected using the technique described in Section II-D. Details are shown in Fig. 4.
7) The committed units are selected using the method mentioned in Section II-B. Table I shows the unit category.

All modeling was done using GAMS 23.7. The computations were carried out using the MILP solver of CPLEX 12.6 on an Intel Xenon 2.55 GHz processor with 32 GB RAM on the Hyak supercomputer system at the University of Washington.

V. Test Results and Sensitivity Analysis

A. Co-Planning versus Independent Planning

Table II shows that co-planning investments in transmission line and BESS capacity significantly reduces the number of lines that must be built.

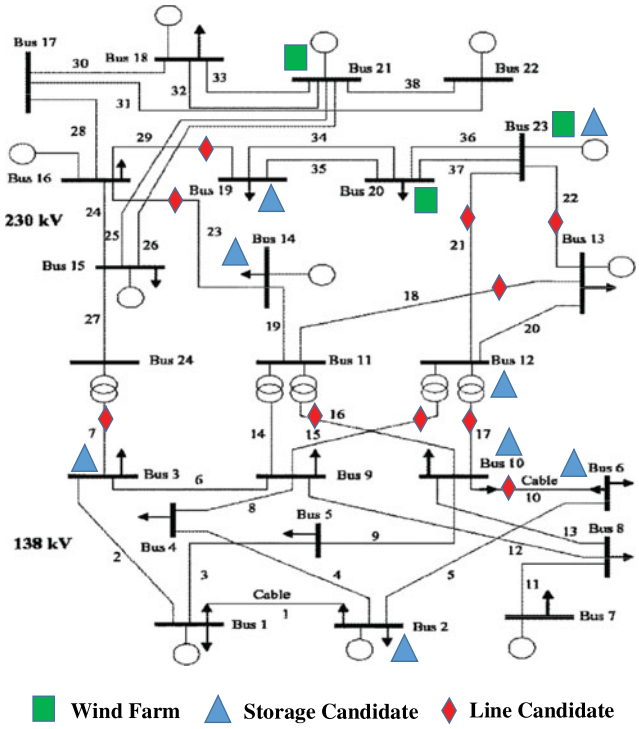

Fig. 4. Test system topology.

TABLE I
UNIT CATEGORY

Type	No	Min-Down (hr)	Min-Up (hr)	Category
1	15–19	1	2	Fast
2	1–2, 5–6	1	2	Fast
3	24–29	1	2	Fast
4	3–4, 7–8	2	3	Slow
5	9–11	2	4	Slow
6	20–21, 30–31	16	24	Slow
7	12–14	3	4	Slow
8	32	5	8	Slow
9	22–23	24	168	Slow

TABLE II
INVESTMENTS IN TRANSMISSION LINE CAPACITY

	Upgraded Lines	Line Capacity(MW)	Construction Start
Co-Planning	Line 21 (buses 12–23)	450	Year 09
Lines Only	Line 29 (buses 16–19)	450	Year 10
	Line 15 (buses 09–12)	360	Year 18
	Line 07 (buses 03–24)	360	Year 19
	Line 18 (buses 11–13)	450	Year 22

Similarly, Table III shows that co-planning the deployment of storage with upgrades in transmission line capacity results in the installation of BESS at fewer locations. However, Fig. 5 shows that the total energy and storage capacities are installed at essentially the same rate, albeit at different locations. As illustrated by Figs. 6 and 7, BESS capacity investments shift from buses at or near wind generation (e.g. buses 14 and 23) to buses close to the load centers (bus 03) to reduce the more expensive load curtailment. Figs. 8 and 9 further illustrate the differences in the timing and the location of the investments recommended by the two planning approaches.

TABLE III
BESS INVESTMENT LOCATION

	BESS Locations
Co-Planning	Bus 3, 6, 10, 12, 19
BESS Only	Bus 3, 6, 10, 12, 14, 19, 23

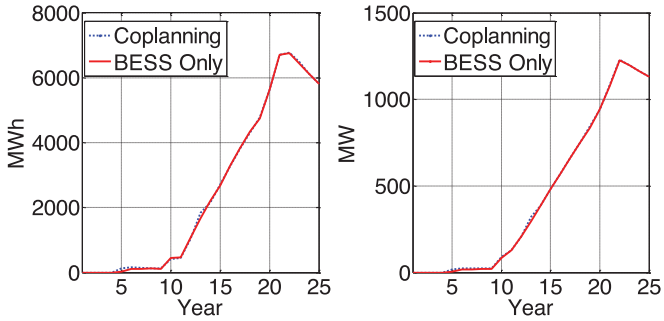

Fig. 5. Total available BESS energy and power capacity as a function of time.

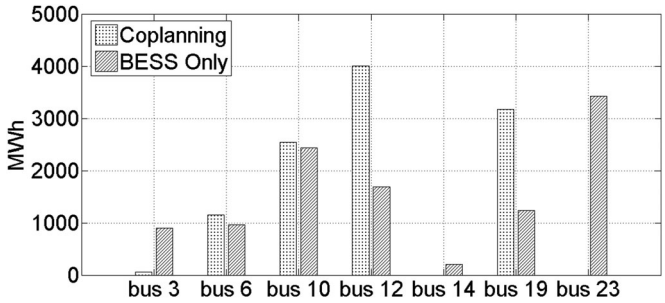

Fig. 6. Total BESS energy capacity installed at each bus.

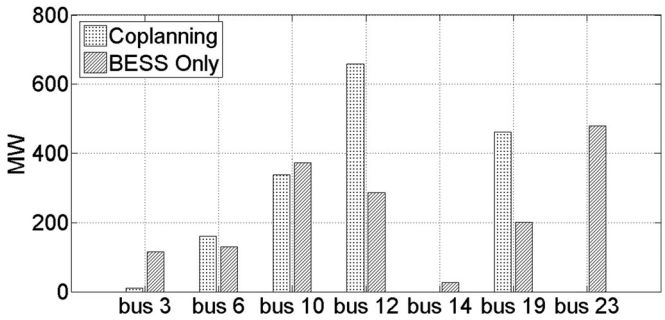

Fig. 7. Total BESS power capacity installed at each bus.

B. Stochastic Optimization

Because long term forecasts of load growth and renewable energy development are inaccurate, considering multiple scenarios and performing the planning using a stochastic optimization

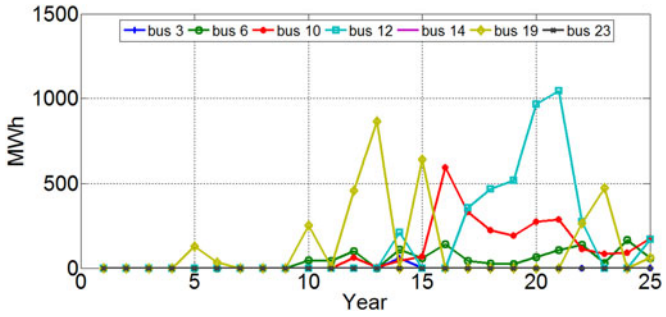

Fig. 8. Energy capacity installed each year at each bus of the planning horizon using the co-planning method.

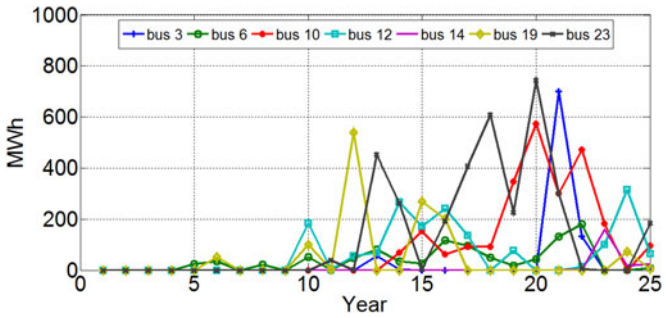

Fig. 9. Energy capacity installed each year at each bus of the planning horizon using the BESS only planning method.

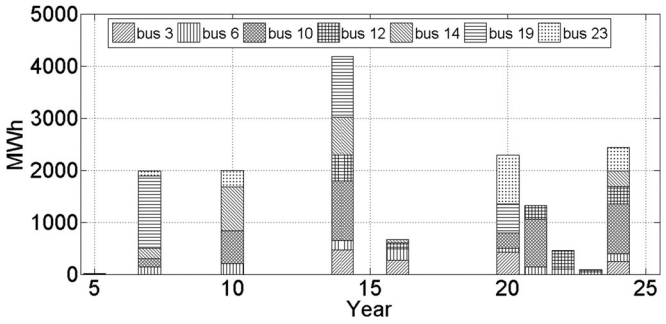

Fig. 10. Total BESS energy capacity installed each year at each bus using stochastic optimization.

provides a more robust investment plan. Fig. 10 shows how much BESS energy capacity should be installed each year at each bus based on a stochastic optimization and the three wind generation and load growth scenarios described in Section II-D. Fig. 11 shows the results obtained with a deterministic optimization using only the base scenario.

Deterministic planning distributes investments in BESS more widely over the years, while stochastic planning recommends larger investments in fewer years. The starting years, capacity at each bus, and total available energy and power capacities are also quite different.

C. *Effect of BESS Lifetime*

The effect of changing the lifetime of each BESS from 10 to 15 years was studied using the co-planning approach. The annualized BESS energy and power capacity costs were changed accordingly, but all other parameters remained the same.

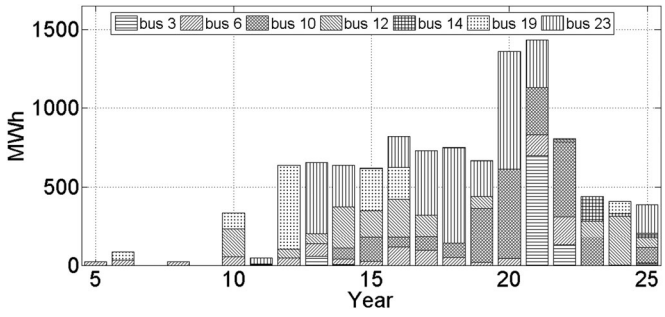

Fig. 11. Total BESS energy capacity installed each year at each bus using deterministic optimization.

TABLE IV
BESS INVESTMENTS

BESS lifetime	BESS Locations
10 years	Bus 3, 6, 10, 12, 19
15 years	Bus 6, 10, 12, 14, 19, 23

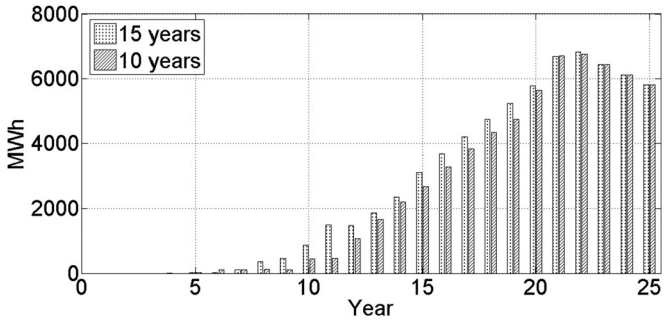

Fig. 12. Total available energy capacity.

TABLE V
LINE CAPACITY UPGRADES

BESS lifetime	Upgraded Lines	Line Capacity(MW)	Construction Year
10 years	Line 21 (bus 12–23)	450	Year 09
15 years	Line 23 (bus 14–16)	450	Year 09
	Line 22 (bus13–23)	450	Year 22
	Line 10 (bus 06–10)	157.5	Year 24

Table IV shows that more BESS are installed when they have a longer lifetime and Fig. 12 that their installation starts sooner. Table V shows that more lines are built when the BESS operate for more years because a longer life time reduces the cost of using BESS and this savings can be used to upgrade more line capacities.

D. *Effect of Transmission Capacity*

To compare the effect of transmission capacity on co-planning, the initial transmission capacity was set to 100%,

TABLE VI
LINE CAPACITY UPGRADES

Initial capacity	Upgraded Lines	Line Capacity(MW)	Construction Year
100%	None	NA	NA
90%	line 21 (bus 12–23)	450	Year 09
80%	Line 22 (bus13–23)	400	Year 07
	Line 29 (bus16–29)	400	Year 11
	Line 10 (bus 6–10)	140	Year 21

TABLE VII
BESS INVESTMENT LOCATION

	BESS Locations
100% Capacity	Bus 06, 10, 12, 14, 19, 23
90% Capacity	Bus 03, 06, 10, 12, 19
80% Capacity	Bus 03, 06, 10, 12, 14, 19, 23

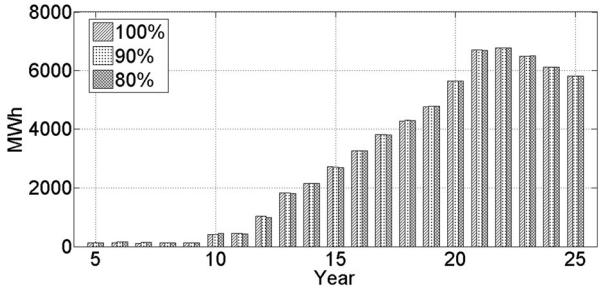

Fig. 13. Available BESS energy capacity for different initial line capacities.

90% and 80% of the original RTS transmission capacity. As one might expect and as Table VI shows, fewer lines need to be upgraded if the initial transmission capacity is larger. On the other hand, as Table VII shows, the locations where BESS are installed change. When less transmission capacity is available, the location of BESS shifts from corridors used to transport wind generation towards load centers (bus 03) to avoid load curtailments and to wind generation centers (bus 23) to reduce wind curtailments.

Fig. 13 shows that the transmission capacity has an almost negligible effect on the total available energy capacities from the BESS installed in the system.

VI. CONCLUSION AND FUTURE WORK

This paper has proposed a stochastic multi-stage method for co-planning transmission and BESS. Compared with the state of art, the proposed method uses more detailed and accurate models over a longer planning horizon. In particular, it takes into account the degradation and limited lifetime of BESS, it considers the reserve constraints and optimizes both the location and capacity of BESS. The size of the problem, and hence the computing burden, remain manageable because generators are grouped by types, and the locations where BESS be installed and the lines that can be upgraded are pre-selected. A sensitivity analysis has been performed to highlight the effect of different planning approaches, of the uncertainty on future load and wind developments, of the BESS lifetime and of the initial transmission capacity.

Over the course of 25 years planning horizon, reserve rate:

$$\frac{\text{Conventional Generation Capacity} + \text{Wind Generation}}{\text{Load Forecast}}$$

will decrease. A negative reserve rate may appears in times when the wind is low and load is high such as in day 3 and 4. Despite the negative reserve rate, the system remain balanced because of the installed BESS. BESS charges during the early hours when the reserve rate is high and discharges during the hours when the reserve rate is low, so part of the capacity has been shifted. In hours when the reserve rate is negative, the BESS virtual generation capacity shifted from the high reserve rate hours is used to keep the system in balance. In the future, there may be significant value in co-planning generation, transmission and BESS to evaluate the benefit of BESS in providing both virtual transmission and generation capacity.

REFERENCES

[1] D. Bertsimas, E. Litvinov, X. Sun, J. Zhao, and T. Zheng, "Adaptive robust optimization for the security constrained unit commitment problem," *IEEE Trans. Power Syst.*, vol. 28, no. 1, pp. 52–63, Mar. 2014.
[2] R. Jiang, J. Wang, and Y. Guan, "Robust unit commitment with wind power and pumped storage hydro," *IEEE Trans. Power Syst.*, vol. 27, no. 2, pp. 800–810, May 2012.
[3] C. Zhao and Y. Guan, "Unified stochastic and robust unit commitment," *IEEE Trans. Power Syst.*, vol. 28, no. 3, pp. 3353–3361, Aug. 2013.
[4] R. Jiang, J. Wang, M. Zhang, and Y. Guan, "Two-stage minimax regret robust unit commitment," *IEEE Trans. Power Syst.*, vol. 28, no. 3, pp. 2271–2282, Aug. 2013.
[5] Y. Wang, Q. Xia, and C. Kang, "Unit commitment with volatile node injections by using interval optimization," *IEEE Trans. Power Syst.*, vol. 26, no. 3, pp. 1705–1713, Aug. 2011.
[6] A. Tuohy, E. Denny, and M. O'Malley, "Rolling unit commitment for systems with significant installed wind capacity," in *Proc. IEEE Lausanne Power Tech Conf.*, 2007, pp. 1380–1385.
[7] T. Qiu, T. Haring, and D.S. Kirschen, "Cost recovery in a rolling horizon unit commitment with energy storage," in *Proc. Power Syst. Comput. Conf. 2014*, 2014, pp. 1–7.
[8] M. Ortega-Vazquez and D.S. Kirschen, "Estimating the spinning reserve requirements in systems with significant wind power generation penetration," *IEEE Trans. Power Syst.*, vol. 24, no. 1, pp. 114–124, Feb. 2009.
[9] A. Papavasiliou, S. Oren, and R. O'Neill, "Reserve requirements for wind power integration: A scenario-based stochastic programming framework," *IEEE Trans. Power Syst.*, vol. 26, no. 4, pp. 2197–2206, Nov. 2011.
[10] K. Bruninx, K. Van den Bergh, E. Delarue, and W. D'haeseleer, "Optimization and allocation of spinning reserves in a low-carbon framework," *IEEE Trans. Power Syst.* , vol. 31, no. 2, pp. 872–882, Mar. 2016.
[11] T. Levin and A. Botterud, "Capacity adequacy and revenue sufficiency in electricity markets with wind power," *IEEE Trans. Power Syst.*, vol. 30, no. 3, pp. 1644–1653, May 2015.
[12] C. Lowery and M. O'Malley, "Reserves in stochastic unit commitment: An Irish system case study," *IEEE Trans. Sustain. Energy*, vol. 6, no. 3, pp. 1029–1038, Jul. 2015.
[13] R. Hemmati, R. Hooshmand, and A. Khodabakhshian, "Comprehensive review of generation and transmission expansion planning," *IET Gener., Transm. Distrib.*, vol. 7, no. 9, pp. 955–964, 2013.
[14] F. Munoz, B. Hobbs, J. Ho, and S. Kasina, "An engineering-economic approach to transmission planning under market and regulatory uncertainties: WECC case study," *IEEE Trans. Power Syst.*, vol. 29, no. 1, pp. 307–317, Jan. 2014.
[15] E. Martinez Cesena, T. Capuder, and P. Mancarella, "Flexible distributed multienergy generation system expansion planning under uncertainty," *IEEE Trans. Smart Grid*, vol. 7, no. 1, pp. 348–357, Jan. 2016.
[16] K. Zach and H. Auer, "Bulk energy storage versus transmission grid investments: Bringing flexibility into future electricity systems with high

penetration of variable RES-electricity," in *Proc. 9th Int. Conf. Eur. Energy Market*, 2012, pp. 1–5.
[17] H. Oh, "Optimal planning to include storage devices in power systems," *IEEE Trans. Power Syst.*, vol. 26, no. 3, pp. 1118–1128, Aug. 2011.
[18] H. Pandzic, Y. Wang, T. Qiu, Y. Dvorkin, and D. S. Kirschen, "Near-optimal method for siting and sizing of distributed storage in a transmission network," *IEEE Trans. Power Syst.*, vol. 30, no. 5, pp. 2288–2300, Sep. 2015.
[19] Y. Liu, W. Du, L. Xiao, H. Wang, and J. Cao, "A method for sizing energy storage system to increase wind penetration as limited by grid frequency deviations," *IEEE Trans. Power Syst.*, vol. 31, no. 1, pp. 729–737, Feb. 2015.
[20] P. Li, R. Dargaville, F. Liu, J. Xia, and Y. Song, "Data-based statistical property analyzing and storage sizing for hybrid renewable energy systems," *IEEE Trans. Ind. Electron*., vol. 62, no. 11, pp. 6996–7008, Nov. 2015.
[21] I. Bayram, M. Abdallah, A. Tajer, and K. Qaraqe, "A stochastic sizing approach for sharing-based energy storage applications," *IEEE Trans. Smart Grid*, to be published.
[22] Z. Hu, F. Zhang, and B. Li, "Transmission expansion planning considering the deployment of energy storage systems," in *Proc. IEEE Power & Energy Soc. General Meeting*, 2012.
[23] F. Zhang, Y. Song, and Z. Hu, "Mixed-integer linear model for transmission expansion planning with line losses and energy storage systems," *IET Gener., Transm. Distrib.*, vol. 7, no. 8, pp. 919–928, 2013.
[24] M. Hedayati, J. Zhang, and K. Hedman, "Joint transmission expansion planning and energy storage placement in smart grid towards efficient integration of renewable energy," in *Proc. IEEE PES T&D Conf. Expo.*, 2014, pp. 1–5.
[25] I. Konstantelos and G. Strbac, "Valuation of flexible transmission investment options under uncertainty," *IEEE Trans. Power Syst.*, vol. 30, no. 2, pp. 1047–1055, Mar. 2015.
[26] S. Chen, K. Tseng, and S. Choi, "Modeling of lithium-ion battery for energy storage system simulation," in *Proc. Asia-Pacific Power Energy Eng. Conf.*, 2009, pp. 1–4.
[27] N. Watrin, H. Ostermann, B. Blunier and A. Miraoui, "Multiphysical lithium-based battery model for use in state-of-charge determination," *IEEE Trans. Veh. Technol.*, vol. 61, no. 8, pp. 3420–3429, Oct. 2012.
[28] P. Fortenbacher, J. Mathieu, and G. Andersson, "Modeling, identification, and optimal control of batteries for power system applications," in *Proc. Power Systems Comput. Conf.*, 2014, pp. 1–4.
[29] *Case Note World's Largest Battery Energy Storage Syst. Fairbanks, AL, USA*. ABB. [Online]. Available: https://library.e.abb.com/public/3c4e15816e4a7bf1c12578d100500565/Case_Note_BESS_GVEA_Fairbanks-web.pdf
[30] *Western Wind and Solar Integration Study*. (2010). National Renewable Energy Laboratory, *Golden*, *CO*, *USA* [Online]. Available: http://www.nrel.gov/docs/fy10osti/47434.pdf
[31] Z. Hu, S. Zhang, F. Zhang, and H. Lu, "SCUC with battery energy storage system for peak-load shaving and reserve support," in *Proc. IEEE Power & Energy Soc. General Meeting*, 2013, pp. 1–4.
[32] [Online]. Available: http://www.ee.washington.edu/research/real/real_pe.html
[33] *Capital Costs for Transmission and Substations: Updated Recommendations for WECC Transmission Expansion Planning*. Western Electricity Coordinating Council. (2014). [Online]. Available: https://www.wecc.biz/Reliability/2014_TEPPC_Transmission_CapCost_Report_B+V.pdf

Ting Qiu (S'12) received the B.S. degree in control science and engineering from Xian University of Technology, China, in 2008 and the M.Sc. degree in system engineering from Xian Jiaotong University, China, in 2011. She is currently pursuing the Ph.D. degree in electrical engineering at the University of Washington, Seattle, WA, USA.

Her research interests include optimization algorithms and their applications in electric power system planning and operation.

Bolun Xu (S'14) received B.S. degrees in Electrical and Computer Engineering from the University of Michigan, Ann Arbor, USA and Shanghai Jiaotong University, Shanghai, China in 2011, and the M.Sc degree in Electrical Engineering from Swiss Federal Institute of Technology, Zurich, Switzerland in 2014. He is currently pursuing the Ph.D. degree in Electrical Engineering at the University of Washington, Seattle, WA, USA.

His research interests include energy storages, power system operations, and power system economics.

Yishen Wang (S'12) received the B.S. degree from the Department of Electrical Engineering, Tsinghua University, Beijing, China, in 2011. He is currently pursuing the Ph.D. degree in electrical engineering at the University of Washington, Seattle, WA, USA.

His research interests include wind integration, wind forecasting, optimization techniques applied to power systems, and power system economics.

Yury Dvorkin (S'11) received the B.S.E.E degree (with the highest Hons.) from Moscow Power Engineering Institute (Technical University), Moscow, Russia, in 2011. He is currently pursuing the Ph.D. degree in electrical engineering at the University of Washington, Seattle, WA, USA.

Previously, he was a Graduate Intern with the Center for Nonlinear Studies, Los Alamos National Laboratory, Los Alamos, NM, USA. His research interests include short- and long-term planning in power systems with renewable generation and power system economics.

Mr. Dvorkin was the recipient of the Clean Energy Institute Graduate Fellowship (2013–2014) and the Clean Energy Institute Student Training and Exploration Grant (2014–2015).

Daniel S. Kirschen (M'86–SM'91–F'07) received the electrical and mechanical engineer's degrees from the Université Libre de Bruxelles, Belgium, in 1979, and the M.Sc. and Ph.D. degrees from the University of Wisconsin, Madison, WI, USA, in 1980 and 1985, respectively. He is currently Close Professor of Electrical Engineering at the University of Washington, Seattle, WA, USA.

His research focuses on smart grids, the integration of renewable energy sources in the grid, power system economics, and power system security.